

## Monte Carlo simulations of Josephson-junction arrays with positional disorder

M. G. Forrester,\* S. P. Benz, and C. J. Lobb

*Department of Physics and Division of Applied Sciences, Harvard University, Cambridge, Massachusetts 02138*

(Received 28 September 1989)

We present the results of Monte Carlo simulations of Josephson-junction arrays with positional disorder, in magnetic fields such that the average number of flux quanta per unit cell is an integer. Granato and Kosterlitz have predicted that such systems should exhibit novel behavior, including a disorder-dependent critical field and a reentrant Kosterlitz-Thouless transition. We find that, for magnetic fields above a field approximately equal to the theoretical critical field, the superconducting phases become essentially randomized for all temperatures, rather than becoming aligned as the temperature decreases. Our results show no clear evidence for a reentrant phase transition in our small ( $16 \times 16$ ) simulated system. These results are consistent with our experiments on proximity-effect arrays with controlled positional disorder. We suggest that the theoretically proposed reentrance is prevented by either finite-size effects or pinning of vortices due to the disorder.

### I. INTRODUCTION

Two-dimensional arrays of Josephson junctions are excellent model systems for the study of various problems in the statistical physics of two-dimensional systems.<sup>1</sup> These problems include the Kosterlitz-Thouless transition, the effects of frustration on phase transitions, commensurate-incommensurate transitions, and the effects of disorder. For example, an array in zero magnetic field provides a realization of a pure  $XY$  magnet, and undergoes a Kosterlitz-Thouless transition, while an array in a finite field is a model for the uniformly frustrated  $XY$  magnet.

Since such arrays can be designed and fabricated in a very controlled way, through the use of photolithography, for example, one has the capability to produce two-dimensional systems with a wide variety of controlled geometries. One can also introduce controlled *disorder* by specifying that certain junctions should not be present in an otherwise regular array. An array with junctions randomly removed provides a realization of a dilute two-dimensional magnet, whose critical behavior may be drastically altered when the disorder becomes sufficiently strong.

In this work we are concerned with arrays whose superconducting sites are given random displacements from the sites of a uniform square lattice. This results in a realization of the  $XY$  magnet with disorder and frustration, which theory suggests may show novel behavior, including a critical value of the disorder, and a reentrant phase transition.

A Josephson-junction array consists of superconducting islands, each characterized by a complex order parameter with phase  $\theta_j$ , connected by Josephson junctions. The Hamiltonian of a uniform array is

$$H = - \sum_{\langle i,j \rangle} J(T) \cos(\theta_i - \theta_j - \psi_{ij}), \quad (1)$$

$$\psi_{ij} = \frac{2\pi}{\Phi_0} \int_i^j \mathbf{A} \cdot d\mathbf{l}, \quad (2)$$

where  $J(T) = \hbar i_c(T)/2e$  is the Josephson energy,  $i_c(T)$  is the critical current of a junction,  $\mathbf{A}$  is the magnetic vector potential,  $\Phi_0 = hc/2e$  is the superconducting flux quantum, and the  $\psi_{ij}$ 's satisfy the constraint

$$\sum_{i,j} \psi_{ij} = 2\pi(m + f) \quad m = 0, \pm 1, \pm 2, \dots, \quad (3)$$

where the summation is around any plaquette. This is the Hamiltonian of a uniformly frustrated  $XY$  magnet, with tunable frustration parametrized by  $f = Bs^2/\Phi_0$ , the number of flux quanta per plaquette, with  $B$  the magnetic field and  $s$  the lattice parameter. The ground-state energy and transition temperature of this system have been shown to be extremely complicated discontinuous functions of  $f$ .<sup>2-4</sup> Measurements of  $T_c$ , resistance, and apparent critical current, as a function of field, in both arrays of junctions<sup>5-9</sup> and wire networks<sup>10</sup> have shown this behavior, albeit somewhat smeared out by sample imperfections. (By "apparent critical current" we mean the current at which the sample voltage exceeds some fixed threshold, usually limited by the sensitivity of the voltmeter. The theoretical zero-voltage critical current is zero in two dimensions at finite temperatures because there is no long-range order).

There are several ways in which samples can be disordered. Consider, for example, a slight generalization of (1), where we allow the Josephson energy  $J$  to vary from junction to junction. We refer to this as *bond disorder* because the strengths of the *bonds* (the junctions) between *sites* (the superconducting islands) vary. This kind of disorder is inevitable in any real array since it is impossible to fabricate samples with all junctions identical. It can be shown theoretically that "weak" bond disorder is irrelevant, and does not affect the critical behavior of the system, while strong enough disorder *can* affect critical exponents.<sup>11</sup> The critical amount of disorder is not known for this system.

Another type of disorder is *site or bond dilution*, where superconducting islands or junctions are removed at random from the lattice. The case of site dilution has been

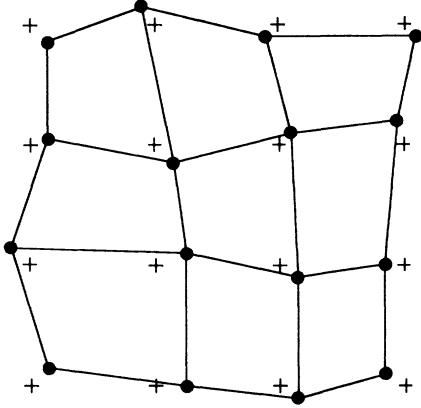


FIG. 1. Schematic diagram of a junction array with positional disorder. Crosses mark the undisplaced positions and solid circles the actual positions of the superconducting islands.

studied theoretically by John and Lubensky,<sup>21</sup> and it has been shown that weak dilution, where only a few percent of the sites are removed, is irrelevant to the critical behavior. On the other hand, these authors showed that strong dilution, where the sample approaches the percolation threshold, can have a dramatic effect, possibly leading to glassy behavior, characterized by extremely slow relaxation to equilibrium.

The third type of disorder one can introduce into the Hamiltonian (1) is randomness in the  $\psi_{ij}$ 's. The natural way to achieve this is to randomize the positions of the superconducting sites, as illustrated in Fig. 1. Clearly this leads to randomness in the plaquette areas (with correlations up to second-nearest-neighbor plaquettes) and therefore to randomness in the frustration  $f$ , giving an  $XY$  model with nonuniform frustration. This kind of disorder is called *positional disorder* and is the topic of this work.

We have previously reported the results of both experiments<sup>13,14</sup> and mean-field calculations<sup>15</sup> for such systems. In this paper we present results of extensive Monte Carlo simulations and renormalization-group calculations for arrays with positional disorder, in magnetic fields such that the *average* number of flux quanta per plaquette,  $f_0$ , is an integer.

The remainder of this paper is organized as follows. In Sec. II we review the predictions of renormalization-group (RG) analysis for arrays with positional disorder. In Sec. III we present the results of our numerical solution of the RG equations. The principal result of this is the detailed shape of the superconducting-normal phase boundary in finite and infinite samples. Section IV presents the results of our Monte Carlo simulations to calculate the specific heat  $C$ , magnetization modulus  $\eta$ , and helicity modulus  $Y$  in such arrays. Finally, Sec. V presents our conclusions.

## II. REVIEW OF RENORMALIZATION-GROUP EQUATIONS

Granato and Kosterlitz (GK)<sup>16</sup> have considered the case where the superconducting sites of an array are dis-

placed from their lattice positions  $\mathbf{r}$  by a random amount  $\mathbf{u}_r$  (expressed as a fraction of the lattice parameter) given by a Gaussian probability density per unit area,

$$P(\mathbf{u}_r) = \frac{1}{2\pi\Delta^2} \exp\left[-\frac{|\mathbf{u}_r|^2}{2\Delta^2}\right], \quad (4)$$

where the parameter  $\Delta$  thus defined quantifies the amount of positional disorder. They showed that the Hamiltonian (1) then describes a gas of fractional charges, interacting with a quenched random distribution of dipoles  $\mathbf{p}_r \propto f_0 \mathbf{u}_r$ .

For the case of  $f_0$  an integer one has a gas of *integral* charges (vortices) perturbed by a random dipole distribution. The nature of these quenched dipoles can be understood by considering a pair of neighboring plaquettes where one bond has been moved a distance  $\delta$  to the right. This produces an area increase (decrease) in the left (right) plaquette proportional to  $\delta$ , and thus, in the Coulomb gas analogy, a pair of charges  $\pm f_0 \delta/s$ , constituting an electric dipole of strength  $f_0 \delta$  (to lowest order in  $\delta$ ).

The problem of a Coulomb gas of *integral* charges perturbed by a random background of dipoles has been studied in another context by Rubinstein, Shraiman, and Nelson.<sup>17</sup> They have derived the recursion relations describing the renormalization of the interaction between a pair of vortices of separation  $r$ , due to both the other vortex pairs and the quenched dipoles. Their results were expressed by Granato and Kosterlitz in terms of arrays with positional disorder as<sup>16</sup>

$$\frac{dK^{-1}(l)}{dl} = 4\pi^3 y^2(l), \quad (5a)$$

$$\frac{dy(l)}{dl} = y(l)[2 - \pi K(l) + 4\pi^3 f_0^2 \Delta^2 K^2(l)], \quad (5b)$$

where  $l = \ln(r/s)$  and  $\Delta$  is the disorder parameter defined by (4). The stiffness  $K(l)$  is related to the energy  $E(l)$  of a vortex pair of separation  $r = s \cdot e^l$  by the relation  $E(l) = \pi k_B T K(l) \ln(r/s)$ , while  $y(l)$ , the vortex fugacity, is related to the density of such vortex pairs.<sup>18</sup> The quantity  $f_0 \Delta$  is effectively the measure of disorder, so that for a sample with fixed  $\Delta$  one can tune the effective disorder by adjusting the magnetic field. When  $f_0 = 0$ , Eq. (5) reduces to the result for the pure case derived by Kosterlitz and Thouless.<sup>18</sup>

The initial conditions from which the renormalization in (5) begins are given by<sup>18</sup>

$$K_o = K(l=0) = J/k_B T, \quad (6a)$$

$$y_o = y(l=0) = \exp(-\pi g K_o), \quad (6b)$$

with  $g = (\frac{3}{2} \ln 2 + \gamma) \approx 1.62$  and  $\gamma \approx 0.577 \dots$  is Euler's constant, as for the pure case. (Henceforth we set  $k_B = 1$ , so that temperatures and energies have the same units).

Following Refs. 16 and 17 we note that there are two special points  $K_{\pm}^{-1}$  where the right-hand side of (5b) vanishes,

$$K_{\pm}^{-1} = \frac{\pi}{4} [1 \pm (1 - 32\pi^3 f_0^2 \Delta^2)^{1/2}], \quad (7)$$

and which divide the solutions of (5) into three regimes. The Hamiltonian flows are sketched in Fig. 2, along with the line of initial conditions  $y = \exp(-\pi g K_0)$  (dotted line). The solid line shows a special trajectory which leaves the  $y=0$  fixed line at  $K_0^{-1}$  and terminates exactly at  $K_+^{-1}$ . The flows *inside* this boundary iterate to  $y(l \rightarrow \infty) = 0$ , and  $K^{-1}(l \rightarrow \infty)$  finite, so that there are no free vortices and the stiffness is finite, just as for  $T < T_c$  in the ordered array. This region is characterized by algebraic decay of correlations, or “quasi-long-range coherence” (QLRC). Outside this region all flows lead to  $y = \infty$  and  $K^{-1} = \infty$  as  $l \rightarrow \infty$ , so that vortices are unbound and the *fully renormalized* stiffness  $K^R = K(l \rightarrow \infty)$  is zero.

Evidently there are now two transition temperatures,  $T_c^-(f_0)$  and  $T_c^+(f_0)$ , as indicated in Fig. 2, at the two points where the locus of initial conditions intersects the critical trajectory (the dark line in Fig. 2). Below  $T_c^-(f_0)$  the quenched dipoles weaken the interaction between the mobile vortices, so that some of the vortices are unbound, and there is no QLRC. This region has no analog in the uniform case where there are no quenched dipoles to weaken the vortex-vortex interaction. For  $T_c^-(f_0) < T < T_c^+(f_0)$ , the increased density of mobile vortices is sufficient to screen the quenched dipoles, so that all the mobile vortices are bound into pairs. Finally, for  $T > T_c^+(f_0)$ , the vortex pairs are thermally unbound, as in a uniform array.

From (7) it is also evident that, for a sample with fixed  $\Delta$ , the special values  $K_{\pm}^{-1}$  merge when  $f_0$  reaches a critical value  $f_c$  given by

$$f_c = \frac{1}{\sqrt{32\pi}} \frac{1}{\Delta} \approx \frac{0.10}{\Delta}. \quad (8)$$

For fields  $f_0 \geq f_c$  the ordered region (inside the solid dark line in Fig. 2) shrinks to zero, and QLRC is destroyed at all temperatures. From Fig. 2 it is also clear that the fully-renormalized stiffness,  $K^R$ , approaches  $K_+$  at both transitions. In contrast to the uniform case this value is *not* universal, since it depends on the magnetic field,  $f_0$ .

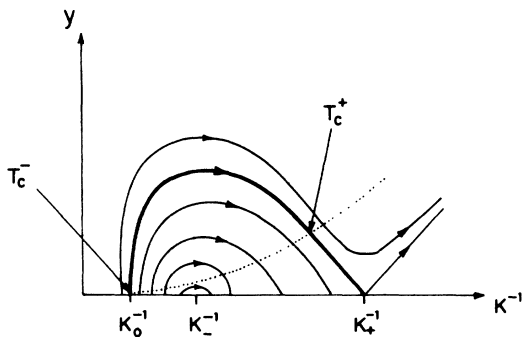


FIG. 2. Renormalization group flows for an array with positional disorder. Flows inside the critical trajectory (solid line) terminate on the critical line  $y=0$ , where there are no free vortices, while those outside diverge towards  $y = \infty$ . There are two vortex-unbinding transitions,  $T_c^+$  and  $T_c^-$ , at the two points where the critical trajectory intersects the line of initial conditions (dashed line).

For  $f_0=0$ , one has  $K_+ = 2/\pi$ , as for the uniform case, while for  $f_0 \rightarrow f_c$ ,  $K_+$  approaches the value  $4/\pi$ .

Examination of the Hamiltonian flows of Fig. 2 also illuminates the importance of finite-size effects. If the integration of Eq. (5) is terminated at a finite value of  $l$ , then the stiffness  $K$  may remain finite even outside the solid line in Fig. 2. This means that in a finite sample the transitions will be smeared out, with the two measured transition temperatures (between which  $K$  is measured to be finite) becoming further apart. This will be demonstrated explicitly in Sec. III.

### III. NUMERICAL SOLUTION OF THE RENORMALIZATION-GROUP EQUATIONS

To gain further insight into the theoretical predictions reviewed above we have numerically solved the renormalization-group equations (5). This enables us to determine the expected shape of the superconducting-normal phase boundary, as well as the behavior of the stiffness,  $K$ , or equivalently the effective superfluid density, as a function of temperature.

We used a fourth-order Runge-Kutta method to integrate (5), starting from the initial conditions (6), to a finite but very large value of  $l, l_f$ , using a step size  $\Delta l$  typically  $10^{-3}$  or  $10^{-2}$ . We also explored the effects of finite sample size by stopping the integration at various small values of  $l$ . To determine  $T_c^+(f_0)$  and  $T_c^-(f_0)$  for the infinite sample we integrated (5) to a large enough value of  $l$  to determine whether a given trajectory (corresponding to a temperature  $T$ ) converged to the fixed line  $y=0$  or diverged to  $y = \infty$ . For temperatures  $T$  far enough from both  $T_c^+(f_0)$  and  $T_c^-(f_0)$  it was often sufficient to take  $l_f=10$ . To determine  $T_c^{\pm}(f_0)$  to a precision of  $0.005J$  it was sufficient to use  $\Delta l = 10^{-3}$  and values of  $l_f$  no larger than 2000.

The resulting phase boundary is shown in Fig. 3. Inside the boundary all vortices are bound in pairs, the fully renormalized fugacity  $y^R = y(l \rightarrow \infty)$  is zero, and the

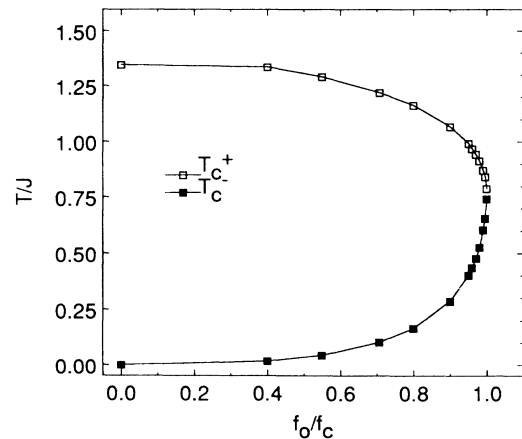


FIG. 3. Theoretical phase boundary, calculated by numerically integrating the renormalization-group equations (5), showing the two transition temperatures  $T_c^{\pm}(f_0)$ . Inside the phase boundary all vortices are bound, while outside some are unbound.

stiffness  $K^R = K(l \rightarrow \infty)$  nonzero. As discussed by Rubinstein, Shraiman, and Nelson,<sup>17</sup> this region is characterized by algebraic decay of spin-spin correlations, or quasi-long-range coherence. The region outside the boundary has  $y^R > 0$  and  $K^R = 0$  and is characterized by exponential decay of correlations.

The temperature dependence of the stiffness at a very large length scale,  $K(l=500)$ , is shown in Fig. 4, for  $f_0/f_c = 0.98$ . Here one directly sees the two transitions at  $T_c^-(f_0)/J \approx 0.5296$  and  $T_c^+(f_0) \approx 0.9156$  at which  $K$  falls to zero. Between the two transitions the RG equations predict that  $KT/J^2$  approaches a value of one. However, spin waves, which are not incorporated in the RG analysis, which explicitly considers only the vortex part of the Hamiltonian, will cause a decrease of this value with increasing temperature. For the pure XY model the leading-order spin-wave correction has been shown to be  $K(T) = K(0)(1 - T/4J)$ .<sup>19</sup> The same correction presumably applies in the presence of disorder.

Figure 4 also shows the result of terminating the integration at  $l = \ln(16) \approx 2.77$ , corresponding to the sample size for the Monte Carlo simulations of Sec. IV. As discussed in Sec. II, this has the effect of smearing the two transitions, and broadening the region in which  $K$  is nonzero.

In summary, there are two striking predictions for the behavior of an infinite Josephson-junction array with positional disorder, in a magnetic field such that the average number of flux quanta per plaquette,  $f_0$ , is an integer. First, there should be two vortex-unbinding transitions, at  $T_c^+(f_0)$  and  $T_c^-(f_0)$ , with the system exhibiting QLRC only for  $T_c^-(f_0) < T < T_c^+(f_0)$ . Second, for fields  $f_0$  greater than a critical value  $f_c$ , given by (8), the two transitions merge, and there is no QLRC at any temperature. In addition, the magnitude of the superfluid jump at both transitions is nonuniversal, depending on the magnetic field  $f_0$ . These predictions still hold for finite

arrays, but with the transitions somewhat broadened by finite-size effects.

Experiments on  $50 \times 50$  proximity-effect arrays have yielded strong support for the critical field (8), but have shown no evidence for reentrant superconductivity.<sup>13,14</sup> However, through Monte Carlo simulation one is able to consider arbitrarily small amounts of positional disorder, and thus large critical fields (8) and thereby investigate integer fields arbitrarily close the critical field where the transition temperature  $T_c^-(f_0)$  should be a maximum.

#### IV. MONTE CARLO SIMULATIONS

To gain further insight into the problem of Josephson-junction arrays with positional disorder, we have performed Monte Carlo simulations of the Hamiltonian (1) (Ref. 20), preliminary results of which have been presented previously.<sup>14</sup> We have examined the field region close to the theoretical phase boundary more closely than previous simulations<sup>21</sup> by considering very small values of the disorder parameter  $\Delta$ , and thus large values of the theoretical critical field (8).

The summation in the Hamiltonian (1) is now considered to be over nearest neighbors on an  $L \times L$  square lattice, with periodic boundary conditions. Our gauge choice is the Landau gauge,

$$\mathbf{A} = B_0 x \hat{y} = \frac{\phi_0 f_0}{s^2} x \hat{y}. \quad (9)$$

In this gauge choice (2) becomes

$$\psi_{ij} = 2\pi \frac{f_0}{s^2} \frac{(x_i + x_j)}{2} (y_j - y_i), \quad (10)$$

Where the coordinates of the  $i$ th spin, or center of the  $i$ th superconducting island, are  $(x_i, y_i)$ .

To calculate quantities as a function of temperature we have followed an annealing schedule in which we started at high temperature,  $T/J \approx 2$ , and then gradually “cooled down” in 20–25 temperature decrements. At the highest temperature we used a random spin configuration as initial condition, while for each successive lower temperature we used the final configuration from the previous higher temperature as input.

At each temperature we executed 5000 Monte Carlo Steps per Spin (MCSS) for equilibration, and 10000 MCSS for averaging. Although it is impossible to know *a priori* how long an equilibration is necessary, we note that Fernández *et al.*<sup>22</sup> have found from their simulations that the *pure XY* model appears to exhibit a size-dependent relaxation time  $\tau_L$ , which follows the form  $\tau_L(\text{MCSS}) \approx 2L^2$ . For our simulations, with  $L = 16$ , this gives  $\tau_L \approx 500$  MCSS, so that our equilibration times are approximately  $10\tau_L$ . The presence of disorder will undoubtedly increase this relaxation time, or possibly even lead to a nonexponential approach to equilibrium. We have found in limited trials, however, that increasing equilibration and averaging times to 50000 and 100000 MCSS, respectively, does not have an appreciable effect on the results. Extensive checks of this kind are impractical due to the large amount of computing time required.

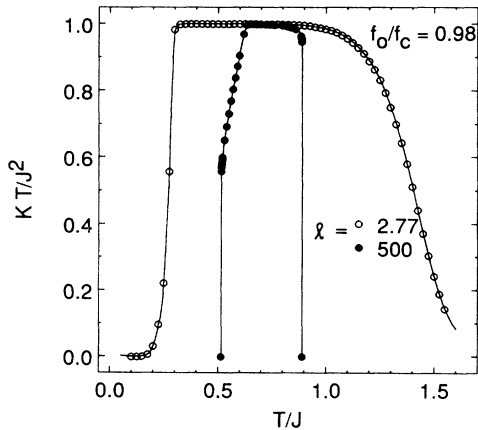


FIG. 4. Results of a numerical calculation of the vortex stiffness,  $K(T)$ , obtained by integrating (5) to length scales of  $l = 2.77$  (corresponding to the Monte Carlo simulated samples) and  $l = 500$  (approximating the infinite sample). For the infinite sample  $K$  drops discontinuously to zero at both transition temperatures, as vortex pairs of separation  $r = s \cdot e^l$  unbind. In the finite sample both transitions become broadened.

### A. Specific heat, $C$

We have calculated the specific heat of our  $L \times L$  spin systems using the relation<sup>23</sup>

$$C = \frac{\langle E^2 \rangle - \langle E \rangle^2}{NT^2}, \quad (11)$$

where  $C$  is the specific heat *per spin*,  $E$  is the total energy of the system calculated from (1),  $N = L^2$  is the number of spins, and  $\langle \dots \rangle$  denotes a combined thermal and configuration average.

The behavior of  $C$  is actually rather uninteresting in the  $KT$  transition, showing only a broad, size-independent peak, at a temperature just above  $T_c$ , with no divergence or cusp. Figure 5 shows results for a value of the Gaussian disorder parameter  $\Delta = 9.9974 \times 10^{-4}$ , so that the theoretical critical field (9) is 100.

The results for  $f_0 = 0$  show a peak at  $T/J \approx 1.1$ , of height  $C \approx 1.5$ , consistent with the simulation results of Tobochnik and Chester.<sup>24</sup> One sees that, as the field is increased, the peak position shifts to lower temperatures and the amplitude decreases, indicating a depression of  $T_c$  by the field. There is however no novel behavior for fields  $f_0 \geq f_c$ , and *no evidence of a second peak associated with a second vortex-unbinding transition*. As shown in the inset in Fig. 5, the position of the peak,  $T_{\text{peak}}$ , simply decreases linearly with field, extrapolating to  $T=0$  at  $f_0 \approx 5.2f_c$ .

### B. Magnetization modulus, $\eta$

A quantity which gives information about the behavior of the phases, or spin angles,  $\theta_i$ , is the magnetization modulus,  $\eta$  (Ref. 25):

$$\eta = \frac{1}{N} \left\langle \left| \sum_{j=1}^N \exp(i\theta_j) \right| \right\rangle. \quad (12)$$

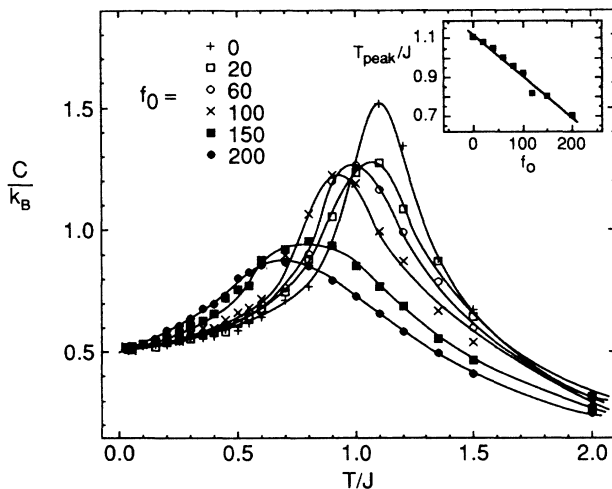


FIG. 5. Specific heat per spin, for a  $16 \times 16$  array, with  $\Delta$  such that  $f_c = 100$ . Inset shows position of the specific heat peak vs magnetic field, showing a linear depression of the peak position. Results are averaged over at least five disorder realizations.

When all the phases are aligned at  $T=0$ , then  $\eta = 1$ , while at high temperatures, where the phases are randomized,  $\eta \approx 1/\sqrt{N}$ , a finite-size-limited value. For the pure  $XY$  model, in zero field, this quantity is considered a reliable measure of long-range order. However, in a finite magnetic field, it is *not gauge invariant*, and therefore is not a measurable quantity. Despite this fact,  $\eta$  turns out to be interesting in its own right.

For a large 2D  $XY$  system, with no disorder,  $\eta(T)$  shows a gradual decrease with increasing temperature, and then a sharp drop to zero at  $T = T_c$ . The behavior for our  $16 \times 16$  system is shown in Fig. 6, where the upper curve is for  $f_0 = 0$ , equivalent to the pure  $XY$  model, and shows a finite-size broadened decay in  $\eta(T)$  in the vicinity of  $T_c \sim J$ .

The other data in Fig. 6 are again for a value of  $\Delta$  such that  $f_c = 100$ . One sees a trend that  $\eta$  is depressed more and more, at all temperatures, as  $f_0$  approaches  $f_c$ . For  $f_0 = f_c = 100$ ,  $\eta(T)$  becomes essentially flat, so that there is *no* development of phase ordering as temperature decreases. This behavior also seems to persist for fields  $f_0 > f_c$  and is further illustrated by Fig. 7, which shows  $\eta(f_0)$  at a fixed temperature  $T/J = 0.5$ , with  $\eta$  decaying to  $1/\sqrt{N} = 1/16 \approx 0.063$  at  $f_0 = f_c = 100$ .

Our interpretation is simply that, as  $f_0 \rightarrow f_c$ , the  $\psi_{ij}$ 's is the Hamiltonian (4.6) essentially all become large compared to  $2\pi$ , so that  $\psi_{ij} \bmod 2\pi$  become essentially uniformly distributed random variables on the interval  $[0, 2\pi]$  or  $[-\pi, \pi]$ . The spin-spin coupling, which wants to minimize the gauge-invariant phase differences,  $\theta_i - \theta_j - \psi_{ij}$ , then orients the phase  $\theta_i$  at random angles, so that  $\eta$  retains its high-temperature, finite-size limited value  $1/\sqrt{N}$  at all temperatures. However, this quantity provides no evidence for the theoretically predicted reentrance phase transition.

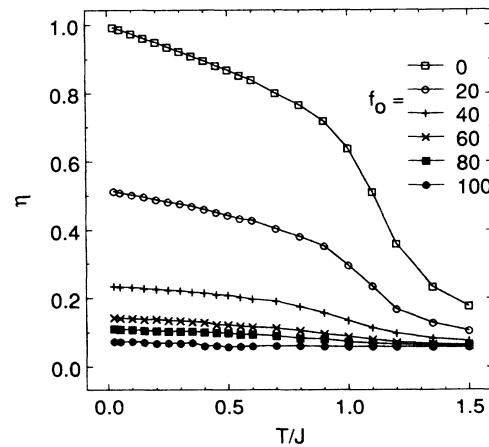


FIG. 6. Magnetization modulus,  $\eta$  vs temperature for various magnetic fields approaching  $f_c = 100$ . Increasing the field suppresses  $\eta$  towards its finite-size value,  $1/\sqrt{N} \approx 0.067$ , indicating that the phases are becoming essentially completely randomized, for fields  $f_0$  of order  $f_c$ . Results are averaged over at least five disorder realizations.

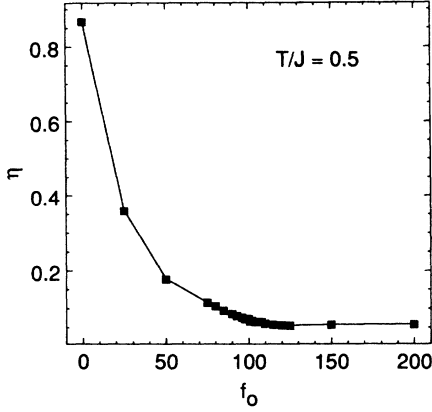


FIG. 7. Results of a simulation at constant temperature  $T/J=0.5$ , showing the field dependence of  $\eta$ , again showing the depression of  $\eta$  towards its finite-size value for fields of order  $f_c$ .

### C. Helicity modulus, $Y$

The helicity modulus,  $Y$ , of a magnetic system is an analog of the shear modulus of a solid. If we take a 2D  $XY$  spin system and cant the phases along one edge, while holding those along the opposite edge fixed, then  $Y$  tells us the increase in free energy of the system in response to the twist induced in the system, in the limit that the wave vector of the twist  $k$  goes to zero. In general  $Y$  is a  $2 \times 2$  matrix (in two dimensions):

$$Y_{ij} = \lim_{k_i, k_j \rightarrow 0} \frac{\partial^2 F}{\partial k_i \partial k_j}.$$

In an isotropic system in equilibrium, the principal component  $Y_{xx} = Y_{yy} = Y$  is simply related to the stiffness  $K$ , by  $Y = KT$ . To calculate  $Y$  we used the expression<sup>26</sup>

$$Y = \frac{1}{N} \sum_{\langle i,j \rangle} J \delta x_{ij}^2 \langle \cos(\theta_i - \theta_j - \psi_{ij}) \rangle - \frac{1}{Nk_B T} \left\langle \left[ \sum_{\langle i,j \rangle} J \delta x_{ij} \sin(\theta_i - \theta_j - \psi_{ij}) \right]^2 \right\rangle + \frac{1}{Nk_B T} \left\langle \sum_{\langle i,j \rangle} J \delta x_{ij} \sin(\theta_i - \theta_j - \psi_{ij}) \right\rangle^2, \quad (13)$$

where  $\delta x_{ij} = x_j - x_i$ , and  $Y$  is the helicity modulus per spin.

In the presence of disorder  $Y$  turned out to be numerically less “well behaved” than the energy, specific heat, and magnetization modulus, exhibiting large fluctuations with temperature for individual disorder realizations. To the extent that constraints on computing power have allowed we have averaged over many (up to 50) disorder realizations, to average such fluctuations.

Figure 8 shows  $Y(T)$  for various values of  $f_0$  in the vicinity of  $f_c = 100$ , averaged over 50 disorder realizations. The results for  $f_0 = 80$  and 120 (20% below and above  $f_c$ , respectively) are qualitatively similar, showing a monotonic increase in  $Y$  with decreasing  $T$ , but with the data for  $f_0 = 80$  showing more downward curvature than that for  $f_0 = 120$ . For  $f_0 = 98$ ,  $Y$  shows a sharp, narrow dip at

$T/J \approx 0.5$ , close to the numerically determined  $T_c^-(f_0)/J \approx 0.5296$  for an infinite lattice. At lower temperatures however,  $Y$  does not go to zero as predicted but increases again as  $T$  decreases, as if some competing mechanism is counteracting any reentrant tendency. For  $f_0 = 99$  the dip at  $T/J \approx 0.5$  is much less evident, while for  $f_0 = 97$  there is no convincing evidence for such a dip.

For fields within a few percent of  $f_c$  the error bars (which represent the variance of  $Y$  over the 50 disorder realizations) are consistently larger than  $T/J=0.5$ , and often near  $T/J=0.3$ . The large error bars in this temperature and field region may be a result of competing mechanisms, one of which causes  $Y$  to decrease and the other  $Y$  to increase, as  $T$  decreases.

Evidently the simulation results obtained for  $Y$  do not support the theoretical prediction illustrated in Fig. 4, where the stiffness  $K$  goes to zero for  $T$  less than some lower transition temperature  $T_c^-(f_0)$ . This may, howev-

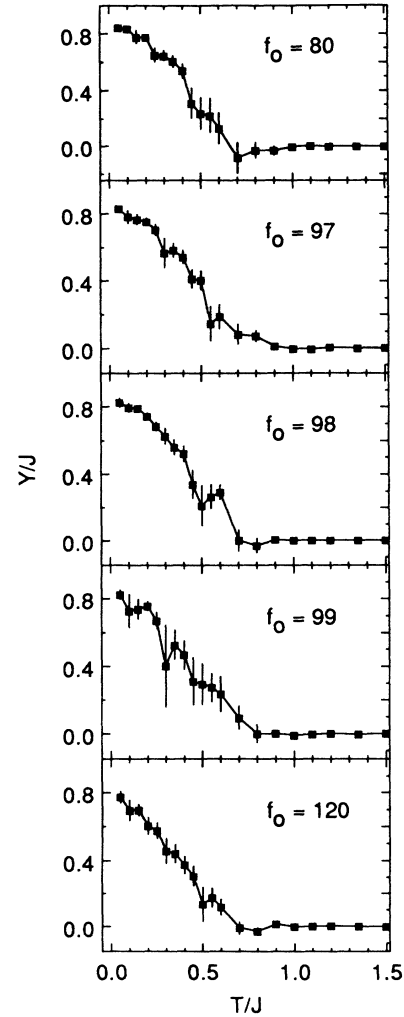


FIG. 8. Helicity modulus  $Y(T)$  for various values of  $f_0$  in the vicinity of  $f_c = 100$ , averaged over 50 disorder realizations, with error bars representing standard deviation of distribution of values of  $Y$  at each  $T$ . Although there is a tendency towards “dips” in  $Y$  near  $T/J=0.3$  and  $0.5$  there is no clear evidence for reentrant behavior.

er, be explained by the small size of the simulated system. We recall that, theoretically, the reentrant phase transition at  $T_c^-$  should be brought about by the unbinding of vortex pairs by the quenched random background of dipoles. However, since these vortices are thermally activated, there will be fewer of them present at low temperatures. In a small sample it is possible that there are actually *no* thermally generated vortices present, at least for part of the time. However, for the calculated helicity modulus to be zero there must be free vortices present at all times to destroy the quasi-long-range order.

An alternative explanation for the lack of reentrance is that, even if there are vortices present, they are pinned by the disorder. If the vortices are not mobile then  $Y$  will not go to zero, just as if there were *no* vortices present. The strength of the pinning should increase with the strength of the effective disorder  $f_0\Delta$ . In fact the theoretical treatment reviewed in Sec. II used a continuum approximation which clearly ignores the pinning sites inherent even in the uniform lattice.<sup>27</sup> The behavior in this low-temperature high-disorder regime may be “glassy” in the sense that, if one waited long enough, vortices might be thermally activated out of their pinning sites, but in computable time scales this does not happen and the vortices remain trapped.<sup>14</sup>

This system is formally identical to the 2D random binary mixture of hard spheres (ball bearings) studied experimentally by Nelson, Rubinstein, and Spaepen.<sup>28</sup> The disorder in that case was due to the presence of a random admixture of *larger* spheres, which disrupted translational order. These authors found that when a system with a dilute concentration of large spheres was “quenched” by increasing the density of spheres, dislocations, analogous to our vortices, became trapped by the large spheres. Thus, although the shear modulus of the system should have been zero, the fact that the dislocations were not free to move resulted in the system having a finite shear modulus.

It is possible that a detailed study of spin configurations from our simulations might illuminate the role of trapping in our system. Experimentally one could look for evidence of hysteretic behavior, say in current-voltage characteristics or resistance versus magnetic field, as long as one could study a regime where pinning was not *too* strong. Experiments to date have shown no evidence of such hysteresis.<sup>13,14</sup>

It is clear that the theoretical work of Granato and Kosterlitz provides an oversimplified description of the behavior of a strongly disordered array. The importance of pinning, and the possibility of glassy behavior, are lost in the RG treatment. The predicted reentrance, for which we have seen no convincing evidence in our simulations, has also not been observed experimentally.

## V. SUMMARY AND CONCLUSIONS

To summarize, we have performed Monte Carlo simulations of 2D  $XY$  magnets with nonuniform frustration, which are model systems for Josephson junction arrays

with positional disorder. We have focused on three quantities in particular—the specific heat  $C$ , magnetization modulus  $\eta$ , and helicity modulus  $Y$ .

Our results for the specific heat show that in an array with positional disorder there is a single broad peak, similar to that found in the pure  $XY$  model. The temperature at which this peak occurred was found to decrease linearly with applied field, extrapolating to  $T=0$  at a field  $f_0 > f_c$ . We found no evidence for novel behavior as  $f_0$  approached the critical field  $f_c$ , and no evidence for a second peak associated with a second, low-temperature, vortex-unbinding transition.

The magnetization modulus,  $\eta(T)$ , although not gauge invariant, proved to be a useful measure of the degree of ordering of the phases, or spins, in our particular gauge choice. We found that  $\eta(T)$  was depressed by the magnetic field, and for fields in the vicinity of  $f_c$ , became essentially independent of temperature, and saturated at a finite-size limited value  $\approx 1/\sqrt{N}$ . This showed that, for such large disorder, there was no development of phase ordering, as measured by  $\eta$ , as temperature decreased. However,  $\eta$  shows no evidence for a reentrant phase transition.

As for the existence of a reentrant phase transition, our results for the helicity modulus  $Y$ , which is equal to the effective superfluid density in an array, are inconclusive. Upon disorder averaging, we found only marginal evidence for a small “dip” in  $Y(T)$  at  $T \approx 0.5$  for some fields very close to  $f_c$ . The overall shape otherwise rose monotonically with decreasing temperature for fields  $f_0$  both greater and less than  $f_c$ , with only a change in curvature as  $f_0$  exceeded  $f_c$ . This lack of reentrance is also consistent with the results of experiments on proximity-effect arrays with positional disorder, which showed strong evidence for a critical field, but no evidence for reentrance.<sup>13,14</sup>

Two possible explanations for this lack of reentrance, and for the behavior of  $Y(T)$  for  $f_0 > f_c$ , are finite-size effects and pinning.<sup>14</sup> The finite-size argument says that our small simulated samples may not contain any vortices at low temperatures, so that quasi-long-range order will not be destroyed and  $Y$  will remain finite. The pinning argument says that although there may be free vortices present at low temperatures, they are so well pinned by the disorder that they cannot move around and destroy the order. Similar arguments have been suggested by Chakrabarti and Dasgupta, who also found no evidence for reentrance in their Monte Carlo simulations performed with a coarser magnetic field scale.<sup>21</sup>

## ACKNOWLEDGMENTS

We thank M. Tinkham for useful discussions, and for his critical reading of the manuscript. We are also indebted to R. Westervelt and P. Sokol for providing computer time. This work was supported in part by the National Science Foundation, through Grants Nos. DMR-86-14003 and DMR-89-12927.

- \*Present address: Westinghouse Science and Technology Center, 1310 Beulah Road, Pittsburgh, PA 15235.
- <sup>1</sup>For a review, see, for example, C. J. Lobb, *Physica* **126B**, 319 (1984).
- <sup>2</sup>S. Alexander, *Phys. Rev. B* **27**, 1541 (1983).
- <sup>3</sup>R. Rammal, T. C. Lubensky, and G. Toulouse, *Phys. Rev. B* **27**, 2820 (1983).
- <sup>4</sup>W. Y. Shih and D. Stroud, *Phys. Rev. B* **28**, 6578 (1983).
- <sup>5</sup>R. A. Webb, R. F. Voss, G. Grinstein, and P. M. Horn, *Phys. Rev. Lett.* **51**, 690 (1983).
- <sup>6</sup>M. Tinkham, D. W. Abraham, and C. J. Lobb, *Phys. Rev. B* **28**, 6578 (1983).
- <sup>7</sup>D. Kimhi, F. Leyvraz, and D. Ariosa, *Phys. Rev. B* **29**, 1487 (1984).
- <sup>8</sup>R. K. Brown and J. C. Garland, *Phys. Rev. B* **33**, 7827 (1986).
- <sup>9</sup>B. J. Van Wees, H. S. J. van der Zant, and J. E. Mooij, *Phys. Rev. B* **35**, 7291 (1987).
- <sup>10</sup>B. Pannetier, J. Chaussy, and R. Rammal, *J. Phys. (Paris) Lett.* **44**, L853 (1983).
- <sup>11</sup>A. B. Harris, *J. Phys. C* **7**, 1671 (1974).
- <sup>12</sup>S. John and T. C. Lubensky, *Phys. Rev. Lett.* **55**, 1014 (1985).
- <sup>13</sup>M. G. Forrester, Hu Jong Lee, M. Tinkham, and C. J. Lobb, *Jpn. J. Appl. Phys.* **26**, Suppl. 26-3, 1423.
- <sup>14</sup>M. G. Forrester, Hu Jong Lee, M. Tinkham, and C. J. Lobb, *Phys. Rev. B* **37**, 5966 (1988).
- <sup>15</sup>S. P. Benz, M. G. Forrester, M. Tinkham, and C. J. Lobb, *Phys. Rev. B* **38**, 2869 (1988).
- <sup>16</sup>E. Granato and J. M. Kosterlitz, *Phys. Rev. B* **33**, 6533 (1986).
- <sup>17</sup>M. Rubinstein, B. Shraiman, and D. R. Nelson, *Phys. Rev. B* **27**, 1800 (1983).
- <sup>18</sup>J. M. Kosterlitz and D. J. Thouless, *J. Phys. C* **6**, 1181 (1973).
- <sup>19</sup>T. Ohta and D. Jasnow, *Phys. Rev. B* **20**, 139 (1979).
- <sup>20</sup>For a review of Monte Carlo methods, see, for example, *Monte Carlo Methods in Statistical Physics*, edited by K. Binder (Springer, Heidelberg, 1974).
- <sup>21</sup>A. Chakrabarti and C. Dasgupta, *Phys. Rev. B* **37**, 7557 (1988).
- <sup>22</sup>J. F. Fernández, M. F. Ferreira, and J. Stankiewicz, *Phys. Rev. B* **34**, 292 (1986).
- <sup>23</sup>F. Reif, *Fundamentals of Statistical and Thermal Physics* (McGraw-Hill, New York, 1965), p. 242.
- <sup>24</sup>J. Tobochnik and G. V. Chester, *Phys. Rev. B* **20**, 3761 (1979).
- <sup>25</sup>C. Ebner and D. Stroud, *Phys. Rev. B* **25**, 5711 (1982).
- <sup>26</sup>W. Y. Shih, C. Ebner, and D. Stroud, *Phys. Rev. B* **30**, 134 (1984).
- <sup>27</sup>C. J. Lobb, D. W. Abraham, and M. Tinkham, *Phys. Rev. B* **27**, 150 (1983).
- <sup>28</sup>D. R. Nelson, M. Rubinstein, and F. Spaepen, *Philos. Mag. A* **46**, 105 (1982).